LEADER-FOLLOWER FORMATION CONTROL OF MULTI-ROBOTS BASED ON BEARING-ONLY OBSERVATIONS

Qing Han,*,** Shudong Sun,** and Hao Lang**

Abstract

This study proposes the bearing-only leader-follower formation control method and examines the nonlinear observability properties of the leader robot system. A study of the nonlinear observability properties between the leader robot and landmarks shows that the system is completely observable when the leader robot can observe four different landmarks. A subsequent study of the leader-follower formation control shows that when the leader robot system satisfies the observability condition of the nonlinear system, the system output can convey sufficient information to allow the observer to provide a correct estimate of the state. Consequently, multi-robots can quickly form and maintain a formation based on the following sufficient bearing-only information, which is that follower robots observe the leader robot. In leader-follower formation, the unscented Kalman filter is employed to estimate the states of the leader-follower robot system. Based on this system, the input-output feedback control law is executed to control the real-time movement of the followers, which allows the leader-follower formation to be properly maintained. Finally, simulation results are presented to demonstrate that the proposed approach can efficiently control the formation of multi-robots as desired.

Key Words

Multi-robots, bearing-only, formation control, unscented Kalman filter

1. Introduction

Multi-robot formation can be employed for various tasks, such as underwater or outer space exploration, shop floor transportation, guarding, escorting, pruning, thinning, harvesting, mowing, spraying, weed removal, and patrolling missions [1]–[4], which has received immense attention from both academics and corporate executives, leading to rapid and significant progress. The advantages of a multi-robot over a single robot system include greater flexibility, adaptability and robustness [5]–[10]. However, controlling multi-robots formation is both challenging and critical, especially when the observation information is poor. A variety of formation control methods have been proposed, such as virtual structure approach [11], [12], behaviour-based approach [13], leader-follower approach [14]–[19], artificial potential [20], [21] and graph theory [22], [23]. Among these, the leader-follower approach has been widely used due to its simplicity, scalability, flexibility, adaptability and reliability. Among the existing leader-follower approaches, most need at least distance-angle information or other information.

In real environments, the available observations of multi-robots might only be bearing observations, which will pose a great challenge to formation control. For the robot formation control, the leader robot plays a very important role. When the leader robot system is observable, the leader-follower formation can run along a complex trajectory and maintain the desired formation. In [23], the number of landmarks is needed for full observability of a group of n robots performing cooperative localization when the robot and landmarks are not on the same line. In [24], the observability analysis of the cooperative location for two robots is presented, with bearing-only measurements, and the robot states are not observable with respect to a global reference frame. It has been shown that two landmarks are needed for the observability of a single vehicle [25]–[27]. Until now, only a few special cases specific to the problem of bearing-only formation control have been solved. In [28]–[30], bearing-only control laws have special requirements for the number of robots, and guaranteed global stability is only applicable to formations composed of three or four robots. In [31], the localization problem using bearing-only observations is studied using a new observability condition valid for general nonlinear systems and based on the extended output Jacobian.

For the formation errors and the speed errors to be bounded, the system must be observable, and the estimation techniques must be used. Recently, some estimation algorithms such as particle filter (PF) [32]–[34], unscented Kalman filter (UKF) [35], the extended Kalman filter [36]

* School of Robot Engineering, Yangtze Normal University, Chongqing 408100, China; e-mail: hanqing@mail.nwpu.edu.cn
** School of Mechanical Engineering, Northwestern Polytechnical University, Xi'an 710072, China; e-mail: sdsun@nwpu.edu.cn, langhao@mail.nwpu.edu.cn
Corresponding author: Qing Han

Recommended by Prof. Anmin Zhu
(DOI: 10.2316/J.2019.206-4831)

and the extended information filter [37] have been used to solve the localization.

Given that car-like robots have better adaptability than unicycle robots in unstructured environment, car-like robot formation is more widely used. Although current research predominantly focuses on unicycle robot formation, car-like robot formation based on bearing-only observations is studied in this paper. Considering the fact that multi-robots are needed to maintain a desired formation in applications such as surveillance, reconnaissance, search and rescue, and transportation, car-like robot formation research has a significant economical and social impact.

In this paper, our approach applies to the situation of n robots. The contribution is threefold. To begin, the car-like robot is front-wheel driving, thus the car-like robot becoming jammed does not occur when the steering angle is $\pm\pi/2$. Meanwhile, the off-axis problem [18], [31] and the singular of the decoupling matrix [14], [31] are both overcome when the follower robots observe the bearing information of the leader robot. Second, observability of the leader robot system is ensured if the leader robot can observe a minimum of two different landmarks. The leader robot's trajectories, which must be ideal in formation control, are overcome using the PF estimation algorithm. Finally, based on the bearing-only observations, UKF is employed for the state estimation of the leader-follower robot formation system, which enables the real-time and stable movement of the follower robots *via* the input-output feedback control.

The remainder of the paper is organized as follows. Section II presents a solution to the leader robot localization problem, which involves the use of PF based on bearing-only observations of landmarks made by the leader robot. Section III presents UKF-based input-output feedback control. Simulation results are given in Section IV. In Section V, we offer our conclusions.

2. The Leader Robot Localization Based on Bearing-only Observations

2.1 Modelling

The setup, we will consider throughout this work, is for n car-like robots. As depicted in Fig. 1, for simplicity, we assume that the two wheels on each axle (front and rear) collapse into a single wheel located at the midpoint of the axle. The front wheel can be steered and driven.

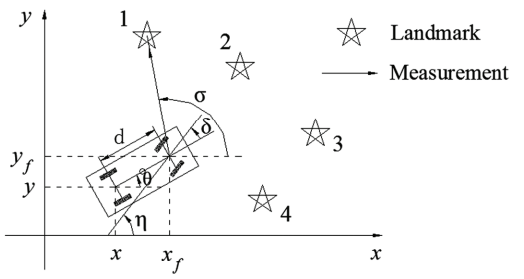

Figure 1. Relative position measurement graph.

The system is subject to two nonholonomic constraints: (1) for the front wheel, and (2) for the rear wheel

$$\dot{x}_f \sin(\delta+\theta) - \dot{y}_f \cos(\delta+\theta) = 0 \tag{1}$$

$$\dot{x}\sin\theta - \dot{y}\cos\theta = 0 \tag{2}$$

The ith front-wheel driving and steering robot kinematics can be abstracted as

$$\dot{S}_i = f_i(S_i,u_i) \triangleq \begin{pmatrix} \dot{x}_{f_i} \\ \dot{y}_{f_i} \\ \dot{\eta}_i \\ \dot{\theta}_i \end{pmatrix} = \begin{pmatrix} \cos\eta_i \\ \sin\eta_i \\ 0 \\ \sin(\eta_i-\theta_i)/d \end{pmatrix} \nu_i + \begin{pmatrix} 0 \\ 0 \\ 1 \\ 0 \end{pmatrix} \omega_i \tag{3}$$

where $S_i = \begin{bmatrix} x_{f_i} & y_{f_i} & \eta_i & \theta_i \end{bmatrix}^{\mathrm{T}} \in \mathbb{R}^4$ is the robot state in the Cartesian coordinates, including the robot position $\begin{bmatrix} x_{f_i} & y_{f_i} \end{bmatrix}$, the robot orientation is θ_i and the absolute steering angle is $\eta_i = \theta_i + \delta_i$ with respect to the x-axis, ν_i and ω_i are the driving and steering velocity, respectively, and d is the distance between the centre of the front and rear axles of the robot. Without loss of generality, we assume that robots can only move forward $\Big(\nu_i \geq 0, \quad i = 1,\cdots,n\Big)$. The ith rear-wheel driving and front-steering robot kinematics can be abstracted as

$$\dot{S}_i = f_i(S_i,u_i) \triangleq \begin{pmatrix} \dot{x}_i \\ \dot{y}_i \\ \dot{\theta}_i \\ \dot{\delta}_i \end{pmatrix} = \begin{pmatrix} \cos\theta_i \\ \sin\theta_i \\ \tan\delta_i/d \\ 0 \end{pmatrix} \nu_i + \begin{pmatrix} 0 \\ 0 \\ 0 \\ 1 \end{pmatrix} \omega_i \tag{4}$$

From (4), we can easily find that there is a model singularity at $\delta_i = \pm\pi/2$, but the singularity does not occur in (3); in fact, the robot can still pivot about its rear wheel at $\delta_i = \pm\pi/2$. Because front-wheel driving robots overcome singularity, we choose the front-wheel driving and steering robots. We assume that each robot uses an exteroceptive sensor to measure relative bearing to other robots and known landmarks that are within the field-of-view of the sensor. Relative bearing from the ith robot to the kth robot or landmark can be written as

$$\vartheta_{ik} = \arctan\left(\frac{y_k - y_{f_i}}{x_k - x_{f_i}}\right) - \eta_i = \sigma_i - \eta_i \tag{5}$$

For leader robot system localization, the leader robot can obtain bearing measurements by measuring four different landmarks.

2.2 Leader Robot Localization using PF

To improve localization accuracy, the position estimation of the leader robot is absolutely critical. We use PF to implement the bearing-only leader robot system location.

In Bayesian terms, the PF approximates the states using a set of random particles with associated non-negative weights:

$$P(s_t) \approx \sum_{i=1}^{N_t} \omega_t^{(i)} \delta_{s_t^{(i)}}(s_t), \quad \sum_{i=1}^{N_t} \omega_t^{(i)} = 1, \quad \omega_t^{(i)} \geq 0 \quad (6)$$

where $\{s_t^{(i)}, \omega_t^{(i)}\}_{i=1,2,\ldots,N_t}$ represent, the states and weights of particles, N_t is the total number of particles at time t and $\delta_s(\cdot)$ denotes the delta-Dirac mass located in the s. The weights ω_t are chosen using the principle of sequential importance sampling (SIS), which relies on

$$\omega_t \propto \omega_{t-1} \frac{p(\vartheta_{ik_t}|s_t)p(s_t|s_{t-1})}{q(s_t|s_{1:t-1}, \vartheta_{ik_t})} \quad (7)$$

where ϑ_{ik_t} is the observation, and $q(\cdot)$ is a proposal importance density.

It is well known and has been verified that after a few iterations in the particle propagation process, the PF will result in sample degeneracy, as depicted [38]. This is one of the inherent faults of SIS. To overcome this, resampling is usually applied [33], [39], which eliminates particles that have small weights and concentrates on particles with large weights, as described by the equation:

$$p(s_t) \approx \sum_{i=1}^{N} \frac{N^{(i)}}{N} \delta_{s_t^{(i)}}(s_t), \sum_{i=1}^{N} N^{(i)} = N \quad (8)$$

where $N^{(i)}$ is the number of times that the ith particle is sampled. The expectation of the number of times each particle is sampled satisfies the unbiasedness condition:

$$E(N^i|\omega_t^{1:N}) = N\omega_t^{(i)} \quad (9)$$

2.3 Observability Analysis of the Leader Robot System

The leader robot plays a very important role in the leader-follower robot formation control. When the leader robot system is observable, the formation errors are bounded. Under that condition, the leader robot's trajectories are very close to the true trajectories. Based on the nonlinear observability rank criteria [40], we derive the linearly independent rows in the observability matrix for the leader robot by observing a certain number of landmarks and the conditions under which the maximum number of linearly independent rows can be obtained. To compute Lie derivatives, the nonlinear kinematic (3) is changed into the following convenient form:

$$\dot{\boldsymbol{s}}_i = f_{\nu_i}\nu_i + f_{w_i}\omega_i \quad (10)$$

The zeroth-order Lie derivative of any scalar function is the function itself, *i.e.*,

$$L^0 h_k(s,z) = h_k(s,z) \quad (11)$$

The first-order Lie derivative of the function $h_k(s,z)$ with respect to f_{ν_i} is defined as

$$L^1_{f_{\nu_i}} h_k(s,z) = \nabla L^0 h_k(s,z) \cdot f_{\nu_i} \quad (12)$$

Here, ∇ represents the gradient operator and $\cdot$ denotes the vector inner product.

Because $L^1_{f_{\nu_i}} h_k(s,z)$ is a scalar function itself, the second-order Lie derivative of $h_k(s,z)$ with respect to f_{ν_i} is

$$L^2_{f_{\nu_i} f_{\nu_i}} h_k(s,z) = \nabla L^1_{f_{\nu_i}} h_k(s,z) \cdot f_{\nu_i} \quad (13)$$

Higher-order Lie derivatives are computed similarly. Additionally, mixed Lie derivatives are defined. The second-order Lie derivative of $h_k(s,z)$ with respect to f_{ν_j}, given its first derivative with respect to f_{ν_i}, is

$$L^2_{f_{\nu_i} f_{\nu_j}} h_k(s,z) = \nabla L^1_{f_{\nu_i}} h_k(s,z) \cdot f_{\nu_j} \quad (14)$$

Based on the preceding expressions for the Lie derivatives, the observability matrix is defined as the matrix with rows

$$M = [\nabla L^p_{f_{\nu_i},\cdots,f_{\nu_j},f_{\omega_i},\cdots f_{\omega_j}} h_k(s,z)] \quad (15)$$

where $j = 1, \cdots, n$, $i, k = 1, \cdots, n$, $p \in \mathrm{N}$.

Lemma 1: Locally, the system is weakly observable if its observability matrix M, which is constructed by the row vector, has full rank, *e.g.*, in our case rank $(M) = 4n$.

For simplicity, we assume $c\theta_i \triangleq \cos\theta_i$, $s\theta_i \triangleq \sin\theta_i$, $s\eta_i \triangleq \sin\eta_i$, $c\eta_i \triangleq \cos\eta_i$, $c\delta_i \triangleq \cos\delta_i$ and $s\delta_i \triangleq \sin\delta_i$. In (3),

$$f_{\nu_i} = [c\eta_i \quad s\eta_i \quad 0 \quad s\delta_i/d]^{\mathrm{T}} \quad (16)$$

$$f_{\omega_i} = [0 \quad 0 \quad 1 \quad 0]^{\mathrm{T}} \quad (17)$$

The necessary Lie derivatives of $h_k(s,z)$ and their gradients are computed, which allows us to obtain the observability matrix M.

A robot observes a landmark:

The zeroth-order Lie derivative:

$$L^0 h_k(s,z) = \vartheta_{ik_1} = \arctan\left(\frac{y_{k_1} - y_{f_i}}{x_{k_1} - x_{f_i}}\right) - \eta_i \quad (18)$$

and its gradient scaled by $R^2_{ik_1}$ is given by

$$\nabla L^0 h_k(s,z) = [-\Delta y_{ik_1} \quad \Delta x_{ik_1} \quad -R^2_{ik_1} \quad 0] \quad (19)$$

where $\Delta x_{ik_1} = x_{f_i} - x_{k_1}$, $y_{ik_1} = y_{f_i} - y_{k_1}$, and $R^2_{ik_1} = (\Delta x_{ik_1})^2 + (\Delta y_{ik_1})^2$.

The first-order Lie derivatives:

$$L^1_{f_{\nu_i}} h_k(s,z) = c\eta_i + s\eta_i \Delta x_{ik_1} - s\delta_i R^2_{ik_1}/d \quad (20)$$

$$L^1_{f_{\omega_i}} h_k(s,z) = -R^2_{ik_1} \quad (21)$$

with their gradients given by

$$\nabla L^1_{f_{\nu_i}} h_k(s,z) = \begin{bmatrix} -2\Delta x_{ik_1} s\delta_i/d + s\eta_i & -2\Delta y_{ik_1} s\delta_i/d - c\eta_i & -R^2_{ik_1} c\delta_i/d + \Delta x_{ik_1} c\eta_i + \Delta y_{ik_1} s\eta_i & R^2_{ik_1} c\delta_i/d \end{bmatrix} \tag{22}$$

$$\nabla L^1_{f_{\omega_i}} h_k(s,z) = 2\begin{bmatrix} -\Delta x_{ik_1} & -\Delta y_{ik_1} & 0 & 0 \end{bmatrix} \tag{23}$$

Clearly, the gradients of the second-order and higher-order Lie derivatives are linearly dependent on the rows of the observability matrix corresponding to the gradients of the first-order and the lower-order Lie derivatives. As a result, we are able to obtain the following two lemmas on the observability of the bearing-only leader robot system as described so far. We can write the rows of the observability matrix corresponding to ϑ_{ik_1}, whereby a robot observes a landmark, using the gradients of Lie derivatives up to the first order, as

$$M_{ik_1} = \begin{bmatrix} -\Delta y_{ik_1} & \Delta x_{ik_1} & -R^2_{ik_1} & 0 \\ -2\Delta x_{ik_1} s\delta_i/d + s\eta_i & -2\Delta y_{ik_1} s\delta_i/d - c\eta_i & -R^2_{ik_1} c\delta_i/d + \Delta x_{ik_1} c\eta_i + \Delta y_{ik_1} s\eta_i & R^2_{ik_1} c\delta_i/d \\ -2\Delta x_{ik_1} & -2\Delta y_{ik_1} & 0 & 0 \end{bmatrix} \tag{24}$$

Lemma 2: The rank of the observability matrix M_{ik_1} given by (24) is 3 if

1. $V_i > 0$;
2. the robot does not move along the line that joins the robot and the landmark.

Proof: If the robot does not move along the line that joins the robot and the landmark, the M_{ik} matrix in (24), by means of a finite sequence of elementary row operations, can be transformed to its simplified form in (25)

$$M_{ik_1} \Rightarrow \begin{bmatrix} 1 & 0 & 0 & \Delta y_{ik_1} \\ 0 & 1 & 0 & -\Delta x_{ik_1} \\ 0 & 0 & 1 & -1 \end{bmatrix} \tag{25}$$

It is obvious that the three nonzero rows in (25) are linearly independent, and they correspond to the gradients of $L^0 h_k(s,z)$, $L^1_{f_{\nu_i}} h_k(s,z)$ and $L^1_{f_{\omega_i}} h_k(s,z)$. Therefore, the rank of (25) is 3, *i.e.*, rank $(M_{ik_1}) = 3$. Moreover, from Lemma 1, we know that the single robot states are not weakly observable at a local level.

A robot observes at least two different landmarks:

The rank of the observability matrix can be easily obtained in the same way as with Lemma 2.
f_{ν_i} and f_{ω_i} are the same as (16) and (17), respectively. Because a robot observes two different landmarks, $h_k(s,z)$ is defined as

$$h_k(s,z) = \begin{bmatrix} \vartheta_{ik_1} \\ \vartheta_{ik_2} \end{bmatrix} \tag{26}$$

We can write the rows of the observability matrix corresponding to $\begin{bmatrix} \vartheta_{ik_1} \\ \vartheta_{ik_2} \end{bmatrix}$, whereby a robot observes two different landmarks, using the gradients of Lie derivatives up to the first order, as (27).

$$M_{ik_{12}} = \begin{bmatrix} -\Delta y_{ik_1} & \Delta x_{ik_1} & -R^2_{ik_1} & 0 \\ -\Delta y_{ik_2} & \Delta x_{ik_2} & -R^2_{ik_2} & 0 \\ -2\Delta x_{ik_1} s\delta_i/d + s\eta_i & -2\Delta y_{ik_1} s\delta_i/d - c\eta_i & -R^2_{ik_1} c\delta_i/d + \Delta x_{ik_1} c\eta_i + \Delta y_{ik_1} s\eta_i & R^2_{ik_1} c\delta_i/d \\ -2\Delta x_{ik_2} s\delta_i/d + s\eta & -2\Delta y_{ik_2} s\delta_i/d - c\eta_i & -R^2_{ik_2} c\delta_i/d + \Delta x_{ik_2} c\eta_i + \Delta y_{ik_2} s\eta_i & R^2_{ik_2} c\delta_i/d \\ -2\Delta x_{ik_1} & -2\Delta y_{ik_1} & 0 & 0 \\ -2\Delta x_{ik_2} & -2\Delta y_{ik_2} & 0 & 0 \end{bmatrix} \tag{27}$$

Lemma 3: The rank of the observability matrix is 4 if

1. $V_i > 0$;
2. the robot does not move along the line that joins the robot and the landmark;
3. the robot and two landmarks are not on the same line (*i.e.*, $\vartheta_{ik_1} \neq \vartheta_{ik_2}$).

Proof: Meeting the three prerequisite requirements above, the $M_{ik_{12}}$ matrix in (27) can be transformed to the simplified form in (28) by means of a finite sequence of elementary row operations.

$$M_{ik_{12}} \Rightarrow \begin{bmatrix} 1 & 0 & 0 & 0 \\ 0 & 1 & 0 & 0 \\ 0 & 0 & 1 & 0 \\ 0 & 0 & 0 & 1 \\ 0 & 0 & 0 & 0 \\ 0 & 0 & 0 & 0 \end{bmatrix} \tag{28}$$

From the results, we can see that the simplified form of the $M_{ik_{12}}$ matrix has four linearly independent rows; therefore, rank $(M_{ik_{12}}) = 4$. Consequently, from Lemma 1, the single robot states are completely observable.

From Lemma 3, we know that if all of the n robots in the group can directly observe a minimum of two different landmarks, then the system is completely observable (*i.e.*, rank $(M) = 4n$). If a system is weakly observable at a local level, the system output can convey information rich enough to allow the observer to provide a correct estimate of the state, thus effectively improving the leader robot localization. Conversely, a system is not observable means that the output does not convey information rich enough to allow the observer to provide a correct estimate of the state, thus negatively affecting the leader robot localization.

3. Leader-Follower Formation Control of Multi-Robots Based on Bearing-only Observations

3.1 Problem Statement

Based on the observability of the leader robot system (the leader robot observing four different landmarks), this section examines the bearing-only leader-follower formation. We will formulate the bearing-only leader-follower observation model and provide the notations used. As shown in Fig. 2, R_2 follows R_1, and R_3 follows R_2. The control inputs for robots are linear and angular velocities $[\nu_i \quad \omega_i]$, $(i = 1, \ldots, n)$, and input vector $\boldsymbol{U} \triangleq [\nu_1 \quad \omega_1 \quad \nu_2 \quad \omega_2 \quad \nu_3 \quad \omega_3]^{\mathrm{T}}$. ρ_i is the distance from the centroid of the leader to the centroid of the follower, φ_i is the view-angle from the y-axis of the follower to the centroid of the leader-robot, and α_i is the relative orientation between the leader robot and the follower robot, *i.e.*, $\alpha_i \triangleq \theta_i - \theta_j$.

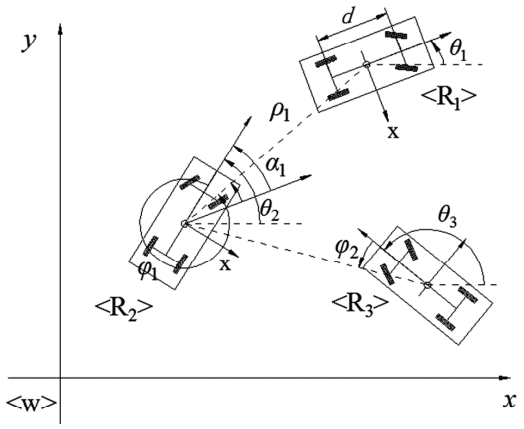

Figure 2. Leader-follower coordinate representation.

With reference to Fig. 2, the kinematic model of a cascade leader-follower robot formation can be expressed as (29)

$$S_n : \begin{cases} \dot{s} = \begin{bmatrix} \dot{\rho}_1 \\ \dot{\varphi}_1 \\ \dot{\alpha}_1 \\ \dot{\rho}_2 \\ \dot{\varphi}_2 \\ \dot{\alpha}_2 \end{bmatrix} = F(s)U = \begin{bmatrix} \cos\delta_1\cos\gamma_1 & 0 & -\cos\delta_2\cos\varphi_1 & 0 & 0 & 0 \\ -\sin\gamma_1\cos\delta_1/\rho_1 & 0 & \cos\delta_2\sin\varphi_1/\rho_1 & -1 & 0 & 0 \\ 0 & 1 & 0 & -1 & 0 & 0 \\ 0 & 0 & \cos\delta_2\cos\gamma_2 & 0 & -\cos\delta_3\cos\varphi_2 & 0 \\ 0 & 0 & -\sin\gamma_2\cos\delta_2/\rho_2 & 0 & \cos\delta_3\sin\varphi_2/\rho_2 & -1 \\ 0 & 0 & 0 & 1 & 0 & -1 \end{bmatrix} \begin{bmatrix} \nu_1 \\ \omega_1 \\ \nu_2 \\ \omega_2 \\ \nu_3 \\ \omega_3 \end{bmatrix} \\ \boldsymbol{y} = h(s) = \left[h_1^{\mathrm{T}}(s), h_2^{\mathrm{T}}(s)\right] \end{cases} \tag{29}$$

where the state vector is $\boldsymbol{s} \triangleq [s_1^{\mathrm{T}}, s_2^{\mathrm{T}}]^{\mathrm{T}}$, $\boldsymbol{s}_1 \triangleq [\rho_1 \quad \varphi_1 \quad \alpha_1]^{\mathrm{T}}$, $\boldsymbol{s}_2 \triangleq [\rho_2 \ \ \varphi_2 \ \ \alpha_2]^{\mathrm{T}}$, $\gamma_i = \varphi_i + \alpha_i \, (i = 1, 2)$, the input vector is $\boldsymbol{U} \triangleq [\nu_1 \ \omega_1 \ \nu_2 \ \omega_2 \ \nu_3 \ \omega_3]^{\mathrm{T}}$, and the output vector is $\boldsymbol{y} = h(s) = \left[h_1^{\mathrm{T}}(s), h_2^{\mathrm{T}}(s)\right]^{\mathrm{T}}$, $h_1 \triangleq [\varphi_1 \ \ \alpha_1]^{\mathrm{T}}$, $h_2 \triangleq [\varphi_2 \ \ \alpha_2]^{\mathrm{T}}$.

The kinematic model of multistage cascade leader-follower robot formation can be readily obtained as an extension of (29).

$$S_n : \begin{cases} \dot{s} = \begin{bmatrix} \dot{\rho}_1 \\ \dot{\varphi}_1 \\ \dot{\alpha}_1 \\ \vdots \\ \dot{\rho}_n \\ \dot{\varphi}_n \\ \dot{\alpha}_n \end{bmatrix} = F(s)U = \begin{bmatrix} \cos\delta_1\cos\gamma_1 & 0 & -\cos\delta_2\cos\varphi_1 & 0 & 0 & 0 \\ -\sin\gamma_1\cos\delta_1/\rho_1 & 0 & \cos\delta_2\sin\varphi_1/\rho_1 & -1 & 0 & 0 \\ 0 & 1 & 0 & -1 & 0 & 0 \\ \vdots & \vdots & \vdots & \vdots & \vdots & \vdots \\ 0 & 0 & \cos\delta_n\cos\gamma_n & 0 & -\cos\delta_{n+1}\cos\varphi_n & 0 \\ 0 & 0 & -\sin\gamma_n\cos\delta_n/\rho_n & 0 & \cos\delta_{n+1}\sin\varphi_n/\rho_n & -1 \\ 0 & 0 & 0 & 1 & 0 & -1 \end{bmatrix} \begin{bmatrix} \nu_1 \\ \omega_1 \\ \nu_2 \\ \omega_2 \\ \vdots \\ \nu_{n+1} \\ \omega_{n+1} \end{bmatrix} \\ \boldsymbol{y} = h(s) = \left[h_1^{\mathrm{T}}(s_1), \quad \ldots, \quad h_n^{\mathrm{T}}(s_n)\right]^{\mathrm{T}} \end{cases} \tag{30}$$

where $\boldsymbol{s} = \left[s_1^{\mathrm{T}}, s_2^{\mathrm{T}}, \cdots, s_n^{\mathrm{T}}\right]^{\mathrm{T}} \in \mathbb{R}^{3n}$ is the state vector, $\boldsymbol{U} = \left[u_1^{\mathrm{T}}, u_2^{\mathrm{T}}, \cdots, u_{n+1}^{\mathrm{T}}\right]^{\mathrm{T}} \in \mathbb{R}^{2(n+1)}$ is the control input vector, output vector $\boldsymbol{y} = h(s) = \left[h_1^{\mathrm{T}}(s_1), \ \ldots, \ h_n^{\mathrm{T}}(s_n)\right]^{\mathrm{T}}$.

3.2 Input-Output Feedback Control Based on UKF

To achieve or maintain a desired leader-follower formation, the followers need to know the relative position of the leader and adjust their current positions accordingly in real time. In our approach, bearing observations are estimated by UKF, and the leader-follower control problem is solved using the classical input-output feedback control law. In the following section, we will explain how to calculate the control input required for the formation of the followers. The control law is designed for R_1 and R_2, which is also similarly designed to other robots of cascade formation.

UKF was implemented to estimate the state $\boldsymbol{s}$ given the input vector U and the output $\boldsymbol{y}$. We assume both the state dynamics (31) and the observation (32) are affected with additive noises as

$$\dot{\boldsymbol{s}} = F(s)U + \mathrm{O} \tag{31}$$

$$\boldsymbol{y} = Gs + N \tag{32}$$

where G is the output transition matrix, O and N are white Gaussian noises with zero mean and covariance matrices P_L and P_N, respectively. We further assume that $\boldsymbol{s}(0)$, O and N are uncorrelated for simplicity. We apply the Euler forward method with sampling time T_c to discretize the state dynamics (31), obtaining

$$s(k+1) = \Gamma(s(k), u(k)) + T_c O \tag{33}$$

where $\Gamma(s(k), u(k)) = T_c F(s)U + s(k)$ and $k \in \mathrm{N}$.

By taking the derivative on $\alpha_1 \triangleq \theta_1 - \theta_2$, we have

$$\dot{\alpha}_1 = \omega_1 - \omega_2 \tag{34}$$

and consider the set of kinematic equations equivalent to the state equation of (29)

$$\dot{\boldsymbol{s}}_{\boldsymbol{r}} = H(s)U_1 + I(s)U_2 \tag{35}$$

where $\boldsymbol{s}_r \triangleq [\rho_1 \ \ \varphi_1]^{\mathrm{T}}$ is the reduced state-space vector, $F_1^{2\times4}$ is the upper-left submatrices of F in (29), $H^{2\times2} = \begin{bmatrix} \cos\delta_1\cos\gamma_1 & 0 \\ -\sin\gamma_1\cos\delta_1/\rho_1 & 0 \end{bmatrix}$ and $I^{2\times2} = \begin{bmatrix} -\cos\delta_2\cos\varphi_1 & 0 \\ \cos\delta_2\sin\varphi_1/\rho_1 & -1 \end{bmatrix}$ are the upper-left and right submatrices of F_1, respectively. It is obvious that the decoupling matrix $I^{2\times2}$ is nonsingular with respect to v_2 and ω_2, *i.e.*, $\det(I^{2\times2}) \neq 0$, so the off-axis problem [18], [31] and singular of the decoupling matrix [14], [31] are both overcome when the follower robots observe the bearing information of the leader robot. The input-output feedback control law [41] algebraically transforms nonlinear system dynamics into linear and then calculates the control input $\boldsymbol{U}$ for the follower to obtain an output state vector $\boldsymbol{s}_r$ converging to a desired s_r^{ide}.

The control input for input-output feedback control system is:

$$\boldsymbol{U}_2 \triangleq [v_2 \quad \omega_2]^{\mathrm{T}} = I^{-1}(s)(C - H(s)U_1) \tag{36}$$

where

$$C = -K(s_r - s_r^{\mathrm{ide}}) \tag{37}$$

and $K = diag\begin{bmatrix} k_1 & k_2 \end{bmatrix}$, with $k_1, \, k_2 > 0$. The superscript "ide" refers to the desired state, and C is the auxiliary

control parameter. Equation (36) serves as a feedback linearizing control for (35). Substituting (36) for (35), the closed-loop dynamics becomes

$$\dot{\boldsymbol{s}}_{\boldsymbol{r}} = C = -K(s_r - s_r^{\text{ide}}) = \begin{bmatrix} k_1(\rho_1^{\text{ide}} - \rho_1) \\ k_2(\varphi_1^{\text{ide}} - \varphi_1) \end{bmatrix}, \ \dot{\alpha}_1 = \omega_1 - \omega_2 \tag{38}$$

4. Simulation Study

This section presents the simulation results to validate the observability conditions regarding the leader robot system discussed in the previous section. For the leader-follower formation system, the simulation environment consists of three robots where R_2 follows R_1, and R_3 follows R_2. To demonstrate the validation of the proposed formation control approach, simulations are designed based on the platform of both Webots 7 and MATLAB. The simulation scenario given in Webots 7 is shown in Fig. 3. In Figs. 4 and 5, the leader robot system performance and the leader-follower formation system performance are given, respectively.

4.1 Initial Conditions

We assume that the noise in this paper is White Gaussian. For the parameters required by the PF, the sampling time is $T_c = 0.01\,\text{s}$, the sample particles are $N_t = 500$, standard deviations of the robot state noise are $[\sigma_{x_{f_i}} \ \sigma_{y_{f_i}} \ \sigma_{\eta_i} \ \sigma_{\theta_i}]^{\text{T}} = [0.05 \ 0.05 \ 0.05 \ 0.05]^{\text{T}}$, and the standard deviation of measure noise is $\sigma_{\vartheta_{ik}} = 0.05$.

Parameters of UKF and the input-output state feedback law are as follows:

We set $\boldsymbol{s}(0) = [0.4474 \ 2.4223 \ 0 \ 0.4360 \ 2.4469 \ 0 \, 0.4126 \ 1.816 \ 0]^{\text{T}}$ and $\boldsymbol{s}_r^{\text{ide}} = [0.45 \ 5\pi/4 \ 0.45 \ 5\pi/4 \ 0.75 \ 5\pi/4]^{\text{T}}$, where distances are in meters and angles in radians. The gains of the controller are $k_1 = 0.25, k_2 = 0.10$. The other parameters of the UKF are $T_c = 0.01\,\text{s}$, $P_L = diag([h \ \ h])$, $P_N = diag([h \ \ h])$, $P = ([1.13 \ \ 1.13])$, where $h = 3.0 \times 10^{-2}\,\text{rad}^2$.

The following velocity inputs have been assigned to the leader robot

$$v_1(t) = 4\,\text{m/s}$$

$$\omega_1(t) = \begin{cases} -\pi/3 & \text{rad/s}, t \in \{[0, 4\} \\ \pi/3 & \text{rad/s}, t \in [4, 7] \\ 0 & \text{rad/s}, t \in 7, 9] \end{cases}$$

The initial configuration vectors of the leader robot and follower robots are

$$\begin{bmatrix} x_1(0) & y_1(0) & \theta_1(0) \end{bmatrix}^{\text{T}} = [0 \quad 0 \quad \pi/4]^{\text{T}}$$

$$\begin{bmatrix} x_2(0) & y_2(0) & \theta_2(0) \end{bmatrix}^{\text{T}} = [-0.1 \quad -0.3 \quad \pi/4]^{\text{T}}$$

$$\begin{bmatrix} x_3(0) & y_3(0) & \theta_3(0) \end{bmatrix}^{\text{T}} = [-0.3 \quad 0.8 \quad \pi/4]^{\text{T}}$$

4.2 Simulation Analysis

In the initial moment, the robots need to adjust the original postures to ideal postures, and the original position error is relatively large. As this has no effect on normal movement of the robot formation, we do not consider position error at the initial moment when all the existing types of simulations are analysed.

The leader robot can obtain bearing measurements by observing different number of landmarks. "0-LM", "1-LM", "2-LM", "3-LM" and "4-LM" represent the number of landmarks, respectively, and are used for leader robot system localization in Fig. 4. Figure 4(a) shows the true and estimated trajectories of the leader robot for each of the five cases. It is evident that the estimated trajectories, which the leader robot can observe using no fewer than two different landmarks, are closest to the true trajectory.

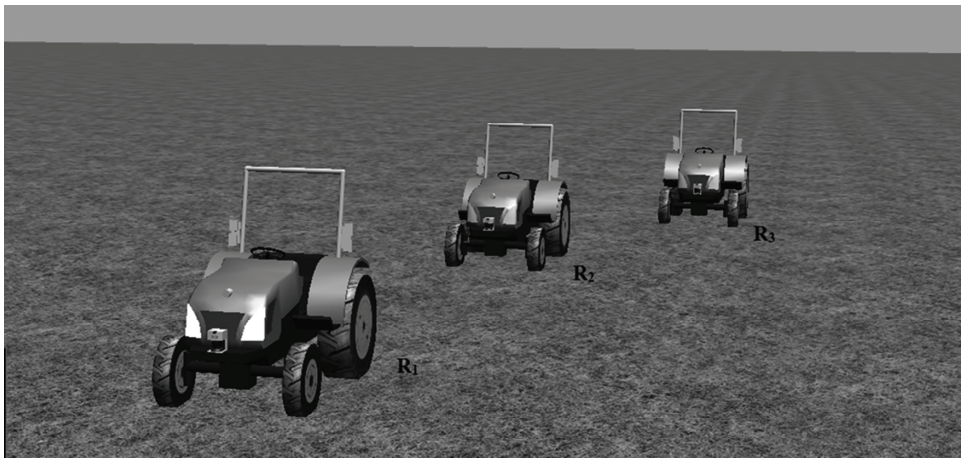

Figure 3. The simulation scene of mobile robots.

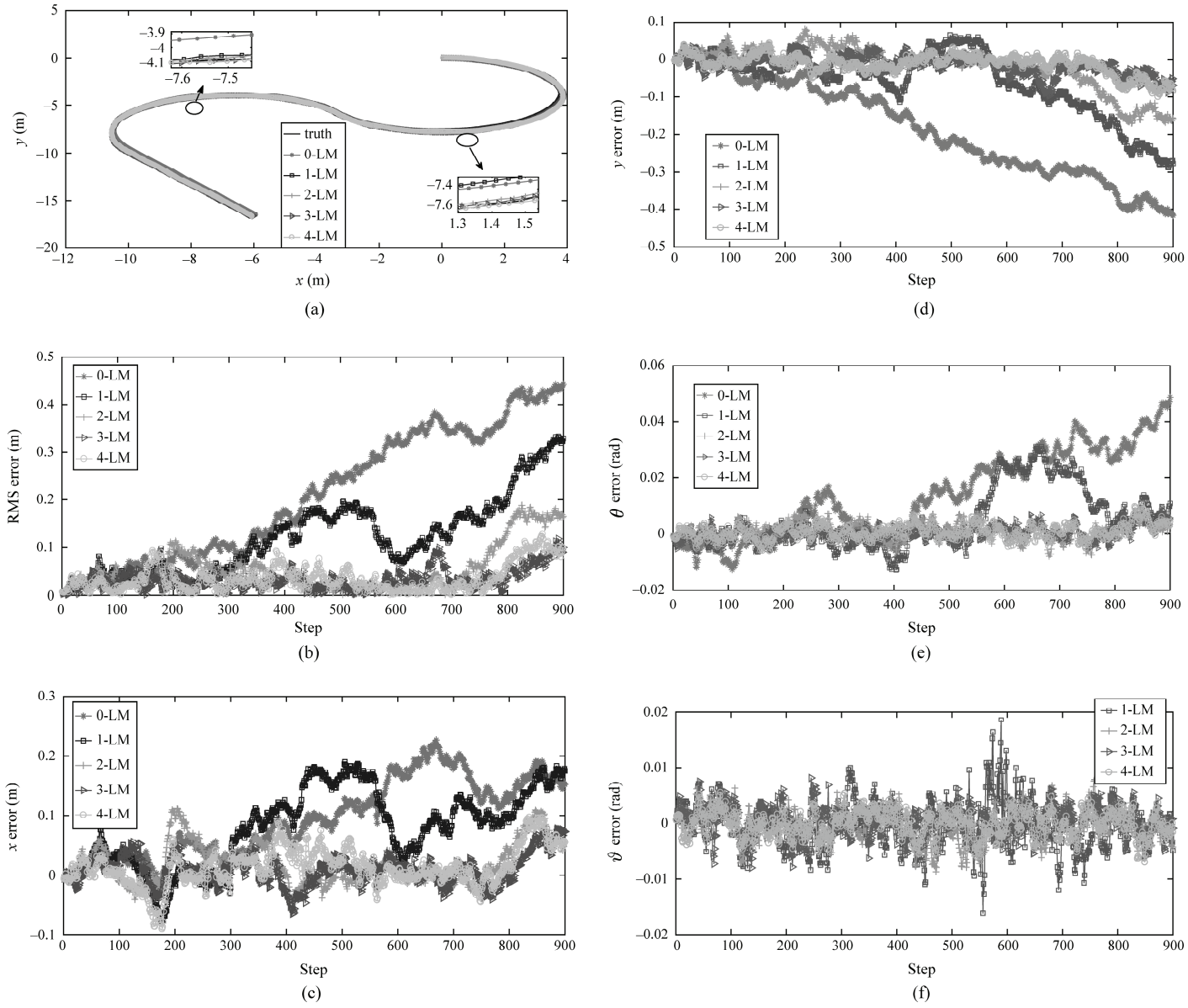

Figure 4. The leader robot system performance: (a) trajectories of the leader robot; (b) root mean square error; (c) error of the leader robot in x direction; (d) error of the leader robot in y direction; (e) orientation error of the leader robot; and (f) observation angle error of the leader robot.

This is because with more than one landmark the leader robot system is observable according to the observability described in Section 2.3. Figure 4(b) shows the plots of the root mean square error with no landmark, one landmark, two landmarks, three landmarks and four landmarks. The root mean square error with either no landmark or one landmark is higher than the error with two, three or four landmarks because, in the last three cases, the leader robot system is observable. Figure 4(c)–(e) shows the plots of error in x, y and θ, respectively, for all five cases, and the error in each case is all small. It is evident that the error for two, three and four landmarks is lower than the error related to no landmark and one landmark. This is because with more than one landmark the leader robot system is observable according to the observability described in Section 2.3. Figure 4(f) shows the plots of relative bearing error for all four cases. Although the relative bearing error for four cases is small, the error for two, three and four landmarks is smaller than the error related to one landmark.

Figure 5(a) gives the trajectories of the leader and followers, showing intuitively that the desired formation is properly formed and maintained. Figure 5(b) shows that the observation angle estimation error is very small. Figure 5(c) shows that the direction angle estimation error is also very small during the input-output feedback control process, except when the leader changes moving direction suddenly from right to left or from left to right, and the maximum direction angle error occurs around -0.0217. Overall, these results indicate a stable performance of the

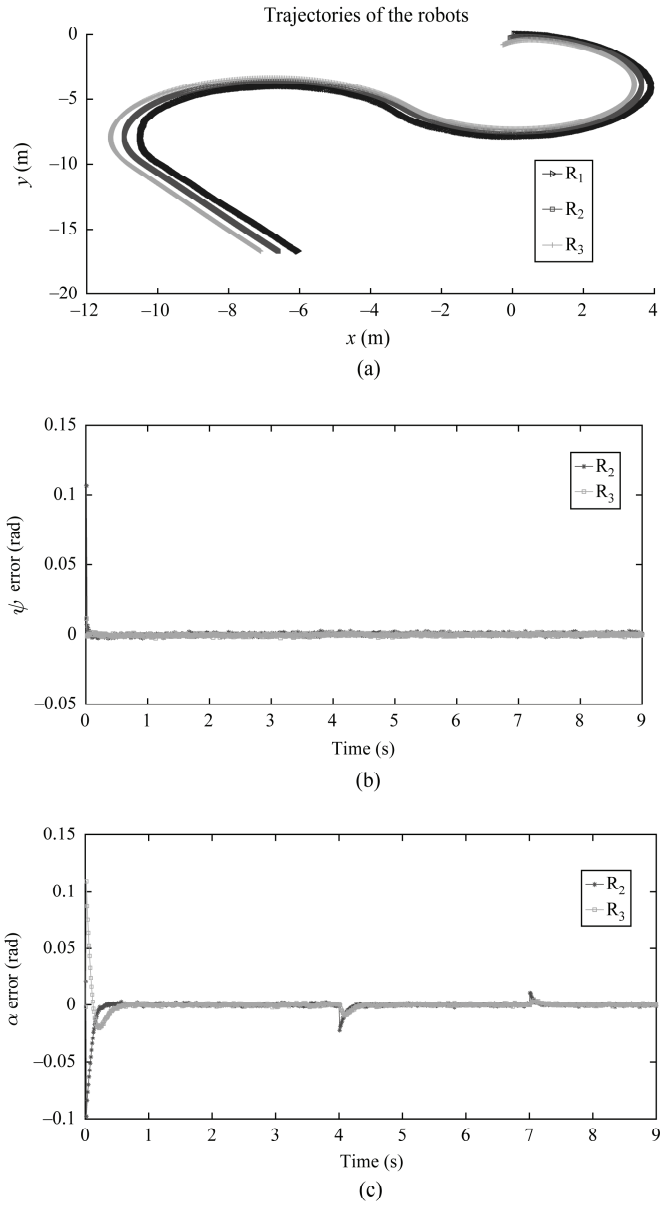

Figure 5. The leader-follower formation system performance: (a) trajectories of robots in Scenario 1; (b) observation angle estimation error; and (c) direction angle estimation error.

proposed formation control solution and a quick response to the change.

5. Conclusion

A new leader-follower formation control method is proposed. Based on the bearing-only observations, the nonlinear observability properties between the leader robot and landmarks are studied. When the leader robot system is observable, the leader-follower formation can rapidly form and remain intact. Simulation results are presented to demonstrate that the proposed approach can efficiently control the formation of multi-robots as desired. Further research for multi-robot formation control will consider dynamical obstacles and formation transformation.

Acknowledgment

This work is sponsored by the National Natural Science Foundation of China (Grant No. 51475383) and the General Program of Yunnan (Grant No. 2017FH001-064).

References

[1] J. Reif and H. Wang, Social potential fields: A distributed behavioral control for autonomous robots, *Robotics and Autonomous Systems*, *27*(3), 1999, 171–194.

[2] L. Barnes, M. Fields, and K. Valavanis, Swarm formation control utilizing elliptical surfaces and limiting functions, *IEEE Transaction on System, Man, and Cybernetics. Part B: Cybernetics*, *39*(6), 2009, 1434–1445.

[3] M. Bergerman, E. van Henten, J. Billingsley, J. Reid, and D. Mingcong, IEEE robotics and automation society technical committee on agricultural robotics and automation, *IEEE Robotics & Automation Magazine*, *20*(2), 2013, 20–125.

[4] C. Luo, A. Zhu, H. Mo, and W. Zhao, Planning optimal trajectory for histogram-enabled mapping and navigation by an efficient PSO algorithm, *Intelligent Control and Automation. IEEE*, Guilin, China, 2016, 1099–1104.

[5] T. Gustavi and X. Hu, Observer-based leader-following formation control using on board sensor information, *IEEE Transaction on Robotics*, *24*(6), 2008, 1457–1462.

[6] H.G. Tanner and J.L. Piovesan, Randomized receding horizon navigation, *IEEE Transaction on Automatic Control*, *55*(11), 2010, 2640–2644.

[7] Z. Peng, G. Wen, and A. Rahmani, Leader-follower formation control of multiple nonholonomic robots based on backstepping, *Proc. 28th Annual ACM Symposium on Applied Computing, ACM*, New York, USA, 2013, 211–216.

[8] X. Yi, A. Zhu, S.X. Yang, and C. Luo, A bio-inspired approach to task assignment of swarm. Robots in 3-d dynamic environment, *IEEE Transactions on Cybernetics*, *47*(4), 2017, 974–983.

[9] A. Zhu and Y. Chen, A machine-learning-based algorithm for detecting a moving object, *International Journal of Robotics & Automation*, *31*(5), 2015, 402–408.

[10] B. Sun, D. Zhu, and S.X. Yang, A bioinspired filtered backstepping tracking control of 7000-m manned submarine vehicle, *IEEE Transactions on Industrial Electronics*, *61*(7), 2014, 3682–3693.

[11] İ. Bayezit and B. Fidan, Distributed cohesive motion control of flight vehicle formations, *IEEE Transactions on Industrial Electronics*, *60*(12), 2013, 5763–5772.

[12] A. Abbaspour, S.A. Moosavian, and K. Alipour, Formation control and obstacle avoidance of cooperative wheeled mobile robots, *International Journal of Robotics and Automation*, *30*(5), 2015, 418–428.

[13] F. Li, Y. Ding, M. Zhou, K. Hao, and L. Chen, An affection-based dynamic leader selection model for formation control in multirobot systems, *IEEE Transactions on Systems Man & Cybernetics Systems*, *47*(7), 2017, 1217–1228.

[14] G. Hassan, K. Yahya, and I. ul Haq, Leader-follower approach using full-state linearization via dynamic feedback, *IEEE International Conference on Emerging Technologies*, Peshawar, Pakistan, 2006, 297–305.

[15] X. Yang, J. Chen, and S.X. Yang, Dynamic bioinspired neural network for multi-robot formation control in unknown environments, *International Journal of Robotics and Automation*, *30*(3), 2015, 256–266.

[16] G. Rishwaraj, S.G. Ponnambalam, and R.K. Chetty, Multi-robot formation control using a hybrid posture estimation strategy, *International Journal of Robotics and Automation*, *29*(4), 2014, 256–266.

[17] D. Atta and B. Subudhi, Decentralized formation control of multiple autonomous underwater vehicles, *International Journal of Robotics and Automation*, *28*(4), 2013, 303–310.

[18] L. Yang, Z. Cao, and C. Zhou, Formation control and switching for multiple robots in uncertain environments, *International Journal of Robotics and Automation*, *25*(3), 2010, 240–249.

[19] H. Wang, D. Guo, X. Liang, W. Chen, G. Hu, and K.K. Leang, Adaptive vision-based leader-follower formation control of mobile robots, *IEEE Transactions on Industrial Electronics*, *64*, 2017, 2893–2902.
[20] P.C. Chen, J. Wan, A.N. Poo, and S.S. Ge, Formation and zoning control of multi-robot systems, *International Journal of Robotics and Automation*, *26*(1), 2011, 35–48.
[21] J.W. Kwon and D. Chwa, Hierarchical formation control based on a vector field method for wheeled mobile robots, *IEEE Transactions on Robotics*, *28*(6), 2012, 1335–1345.
[22] A.I. Mourikis and S.I. Roumeliotis, Performance analysis of multirobot cooperative localization, *IEEE Transactions on Robotics*, *22*(4), 2006, 666–681.
[23] R. Sharma, R.W. Beard, C.N. Taylor, and S. Quebe, Graph-based observability analysis of bearing-only cooperative localization, *IEEE Transactions on Robotics*, *28*(2), 2012, 522–529.
[24] A. Martinelli and R. Siegwart, Observability analysis for mobile robot localization, *Proc. IEEE/RSJ Int. Conf. Intell. Robots Syst.*, Edmonton, Alta., Canada, 2005, 1471–1476.
[25] M. Betke and L. Gurvits, Mobile robot localization using landmarks, *IEEE Transactions on Robotics and Automation*, *13*(2), 1997, 251–263.
[26] L.D.L. Perera, A. Melkumyan, and E. Nettleton, On the linear and nonlinear observability analysis of the SLAM problem, *Proc. IEEE Int. Conf. Mechatronics*, Malaga, Spain, 2009, 1–6.
[27] K.W. Lee, W.S. Wijesoma, and I.G. Javier, On the observability and observability analysis of SLAM, *Proc. IEEE/RSJ Int. Robots Syst. Conf.*, Beijing, China, 2006, 3569–3574.
[28] M. Basiri, A.N. Bishop, and P. Jensfelt, Distributed control of triangular formations with angle-only constraints, *Systems & Control Letters*, *59*(2), 2010, 147–154.
[29] A.N. Bishop, A very relaxed control law for bearing-only triangular formation control, *Proc. 18th IFAC World Congress*, Milano, Italy, 2011, 5991–5998.
[30] A.N. Bishop, Distributed bearing-only quadrilateral formation control, *Proc. 18th IFAC World Congress*, Milano, Italy, 2011, 4507–4512.
[31] G.L. Mariottini, F. Morbidi, D. Prattichizzo, N.V. Valk, and N. Michael, Vision-based localization for leader-follower formation control, *IEEE Transactions on Robotics*, *25*(6), 2009, 1431–1438.
[32] D. Fox, W. Burgard, H. Kruppa, and S. Thrun, A probabilistic approach to collaborative multi-robot localization, *Autonomous Robots*, *8*, 2000, 325–344.
[33] T. Li, M. Bolic, and P. Djuric, Resampling methods for particle filtering, *IEEE Signal Processing Magazine*, *32*(3), 2015, 70–86.
[34] X. Wang, T. Li, S. Sun, and J.M. Corchado, A survey of recent advances in particle filters and remaining challenges for multitarget tracking, *Sensors*, *17*, 2017, 2707.
[35] Q. Han, T. Li, S. Sun, G. Villarrubia, and F. de la Prieta, "1-N" leader-follower formation control of multiple robots based on bearing-only observation", *Advances in Practical Applications of Robots, Multi-Robot Systems, and Sustainability: The PAAMS Collection* (Springer International Publishing, 2015), 120–130.
[36] J. Zhao, M. Netto, and L. Mili, A robust iterated extended Kalman filter for power system dynamic state estimation, *IEEE Transactions on Power Systems*, *32*(4), 2017, 3205–3216.
[37] R. Sharma, S. Quebe, R.W. Beard, and C.N. Taylor, Bearing-only cooperative localization, *Journal of Intelligent & Robotic Systems*, *72*(3–4), 2013, 429–440.
[38] T. Li, S. Sun, T.P. Sattar, and J.M. Corchado, Fight sample degeneracy and impoverishment in particle filters: A review of intelligent approaches, *Expert Systems with Applications*, *41*(8), 2014, 3944–3954.
[39] T. Li, G. Villarrubia, S. Sun, J.M. Corchado, and J. Bajo, Resampling methods for particle filtering: Identical distribution, a new method and comparable study, *Frontiers of Information Technology & Electronic Engineering*, *16*(11), 2015, 969–984.
[40] R. Hermann and A.J. Krener, Nonlinear controllability and observability, *IEEE Transactions on Automatic Control*, *22*(5), 1977, 728–740.
[41] J.J.E. Slotine and W. Li, *Applied Nonlinear Control, vol. 46, no. 1* (Englewood Cliffs, NJ: Prentice-Hall, 1991).

Biographies

Qing Han, Ph.D, was born in China, in 1973. His research interests include intelligent robots, multi-robot coordination control, electromechanical integration and electromechanical control technique.

Shudong Sun was born in China, in 1963, Ph.D, professor, doctoral supervisor. His research interests lie in the areas of the robot and intelligent control, modern integrated manufacturing systems, industrial engineering, *etc.*

Hao Lang was born in China, in 1992, master degree. His research interests lie in the areas of information fusion technology, particle filter and simultaneous localization and mapping.